JOURNAL OF GEOPHYSICAL RESEARCH, VOL. 112, C08003, doi:10.1029/2006JC004033, 2007

Tide-surge interaction and its role in the distribution of surge residuals in the North Sea

K. J. Horsburgh[1] and C. Wilson[1]

Received 29 November 2006; revised 26 February 2007; accepted 8 May 2007; published 3 August 2007.

[1] Storm surges are the sea level response to meteorological conditions. Scientists and engineers need to understand the interaction of surges with the tide in order to provide better estimates of extreme sea level for use in coastal defense. Using data from five tide gauges, spaced equally along the North Sea coastline around the UK, we show that the mode of peak residual occurrence is everywhere 3 to 5 hours before the nearest high water. We reveal a previously unobserved mode that falls 1 to 2 hours prior to high water, although this cluster is not associated with the highest residuals. A simple mathematical explanation for surge clustering on the rising tide is presented. The phase shift of the tidal signal is combined with the modulation of surge production due to water depth in a model that provides a good description of the residual data set. The results contain several features of interest for flood risk management. We show that large, locally generated surges are precluded close to high water. For physically realistic arrival times of any travelling surge component, the residual peak will avoid high water for any finite tidal phase shift. Furthermore, increasing the tidal range reduces the risk of residual peaks near high water. We draw attention to the existence of critical time and space scales for surge development and decay. For reliable operational forecasts of sea level, coastal numerical models need to reproduce both tides and surges with improved accuracy.

Citation: Horsburgh, K. J., and C. Wilson (2007), Tide-surge interaction and its role in the distribution of surge residuals in the North Sea, *J. Geophys. Res.*, *112*, C08003, doi:10.1029/2006JC004033.

1. Introduction

[2] Storm surges are an important component of total sea level and have been the subject of much scientific investigation, particularly in the North Sea where they were a significant factor in the disastrous floods of February 1953 [*McRobie et al.*, 2005]. It is important that marine scientists and engineers have the best possible understanding of surge development, tide-surge interaction and the statistics of surge occurrence over long timescales; then it is possible to combine surge, tide and other factors to provide estimates of extreme sea level for design purposes using statistical techniques [e.g., *Pugh and Vassie*, 1980; *Tawn and Vassie*, 1989]. Since the tidal range around most of the UK coastline is typically of the order of several meters, surges only represent a threat if they are near-coincident with high water. Consequently, research has focused on the process of tide-surge interaction, with the emphasis on estuaries rather than the broader shelf sea.

[3] A tendency for surge maxima in the Thames estuary to occur most frequently on the rising tide has been recognized for a long time [*Doodson*, 1929; *Rossiter*, 1961]. Formal solutions for the propagation of an externally forced tide and surge into an estuary of uniform section were developed by *Proudman* [1955, 1957] who drew conclusions about the impact of shallow water and bottom friction on the timing and magnitude of high water, both for standing and progressive waves. However, his analysis was not sufficiently general to explore the underlying dynamics and neither did his results agree with observations, except in the immediate vicinity of the open boundary condition. In numerical solutions, *Rossiter* [1961] assumed idealized surges with diurnal periodicity and showed how a negative surge would retard tidal propagation whereas a positive surge would advance high water (through a combination of depth affecting the wave propagation speed, and depth-dependent frictional terms in the equations of motion). The analysis was again restricted to an estuary forced dynamically at its mouth, whereas (as we will show here) similar effects are obtained from tide gauge records along the full length of the UK North Sea coastline. *Prandle and Wolf* [1978] looked at tide gauge data from nine ports along the UK east coast for the period 1969–1973. They confirmed the tendency for surge peaks to occur most often on the rising tide, and used numerical models to conclude that this pattern arises irrespective of the phase relationship between tide and surge in the northern North Sea. The models made it possible to separate the contribution to interaction from shallow water and bottom friction. *Wolf* [1981] subsequently used a one-dimensional analytical model to show that the shallow water effect becomes dominant over quadratic friction for tidal amplitudes in excess of 3 m and in depths of 10 m or less.

[1] Proudman Oceanographic Laboratory, Liverpool, UK.

0148-0227/07/2006JC004033$09.00

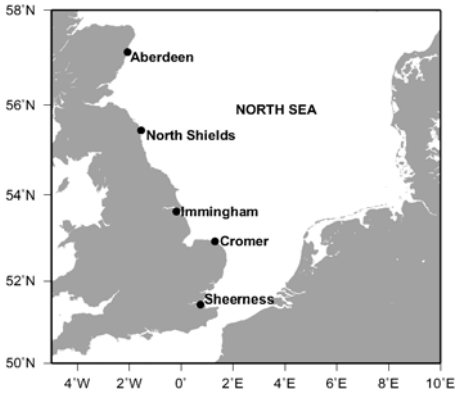

Figure 1. Map of the study area, showing the tide gauge sites from which data were analyzed.

[4] Quality-controlled tide gauge data from all ports in the UK A-Class network from 1915 onward have recently become available. Since 1993, the observations were stored at 15-minute intervals, allowing the calculation of nontidal residuals at improved temporal resolution. It is timely then to (1) review the statistics of surge duration and occurrence with respect to high water and (2) try and provide a better physical explanation for the observed distribution of surges. An important ancillary question is whether it is possible for extreme surges (those exceeding some locally relevant threshold) in the southern North Sea to arrive closer to high water than has historically been the case. This is of great interest to government and coastal engineers because of the proposed redevelopment of the floodplains surrounding the Thames estuary [*Lavery and Donovan*, 2005]. There is no compelling evidence for regional trends in either storm surge frequency or magnitude over recent decades. In a global study of 141 stations, *Woodworth and Blackman* [2004] did find increases in extreme high water levels while *Zhang et al.* [2000] reached a similar conclusion for the US east coast. However, in most cases, the variability in extremes was related to that of mean sea level. The lack of any discernible trend over the last century in the magnitude of nontidal sea level variability around the UK is noted by *Pugh and Maul* [1999]. This study provides part of the background necessary to assess the likelihood of changes to extreme sea level events in the future.

[5] *Rossiter* [1961] suggested that a key mechanism of interaction between the tide and surge is one of mutual phase alteration. We confirm that conclusion in this work and provide a novel but simple mathematical explanation for the majority of observed effects. We begin by reviewing all available data from five tide gauges, spaced equally along the North Sea coastline. Next, a simple model leads to an improved explanation for surge clustering on the rising tide. We then analyze a subset of surges exceeding the 99th percentile at Sheerness to demonstrate that this model holds for larger events. A depth-averaged hydrodynamic model is employed to illustrate how the amount of surge generated depends on the tidal state. Finally, the physical mechanisms of phase alteration and tidally modulated surge production are combined in a simple scheme that is consistent with the residual distribution data set.

2. Analysis of Tide Gauge Data

[6] We analyzed tide gauge data from the five sites on the east coast of the UK shown in Figure 1. The data span the period 1950 until 2005, and nontidal residuals were calculated in the usual way by subtracting harmonic tidal predictions from the observed sea level [*Pugh*, 1987]. Throughout this paper, we use the term "surge" only when implying a genuine meteorological contribution to sea level; otherwise, we refer to "residual", which may contain surge, tide-surge interaction, harmonic prediction errors and timing errors. Data from 1993 onwards were available at 15-minute intervals whereas older data were hourly. Discrete residual events were defined as those that exceeded 25 cm. To avoid double-counting, individual events had to be separated by 12 hours. The data are summarized in Table 1.

[7] Later in the paper, we focus only on positive residuals, since they are of greater practical significance, but in the analysis of tide gauge data, all events were considered, including negative surges. Figure 2 shows the normalized frequency of positive residual events, with respect to the time of the nearest high water, for the five sites. There were no qualitative differences between the histograms of the hourly data prior to 1993 and the more recent 15-minute data, as can be seen by comparing Figures 2a and 2b, or inspecting the modes in Table 1. Indeed, when the Aberdeen data from 1993 to 2005 were resampled at hourly intervals, the histogram was indistinguishable from Figure 2a. Therefore we concentrate on the 1993–2005 data which have better temporal resolution. The magnitudes of residuals are indicated in Figure 2 using color subdivision of the histogram bars as described in Figure 2b.

[8] Our results confirm the previously reported tendency for residuals to occur most frequently on the rising tide. The mode of residual occurrence is everywhere 3 to 5 hours before the nearest high water, but the distributions in Figure 2 contain other features of interest. The frequency patterns are clearly multimodal, with a second, but less dominant, mode on the falling tide. Aberdeen (Figure 2b) has the most

Table 1. Tide Gauge Data Used in This Study

Site	Mean spring tidal range, m	Discrete events (pre-1993)	Discrete events (1993–2005)	Modal residual peak w.r.t. HW (pre-1993)	Modal residual peak w.r.t. HW (1993–2005)
Aberdeen	3.6	996	611	−4	−3.75
North Shields	4.4	1058	742	−4	−4
Immingham	6.2	2618	1067	−5	−4.75
Cromer	4.2	306	1083	−3	−3
Sheerness	5.2	2079	1326	−4	−4.25

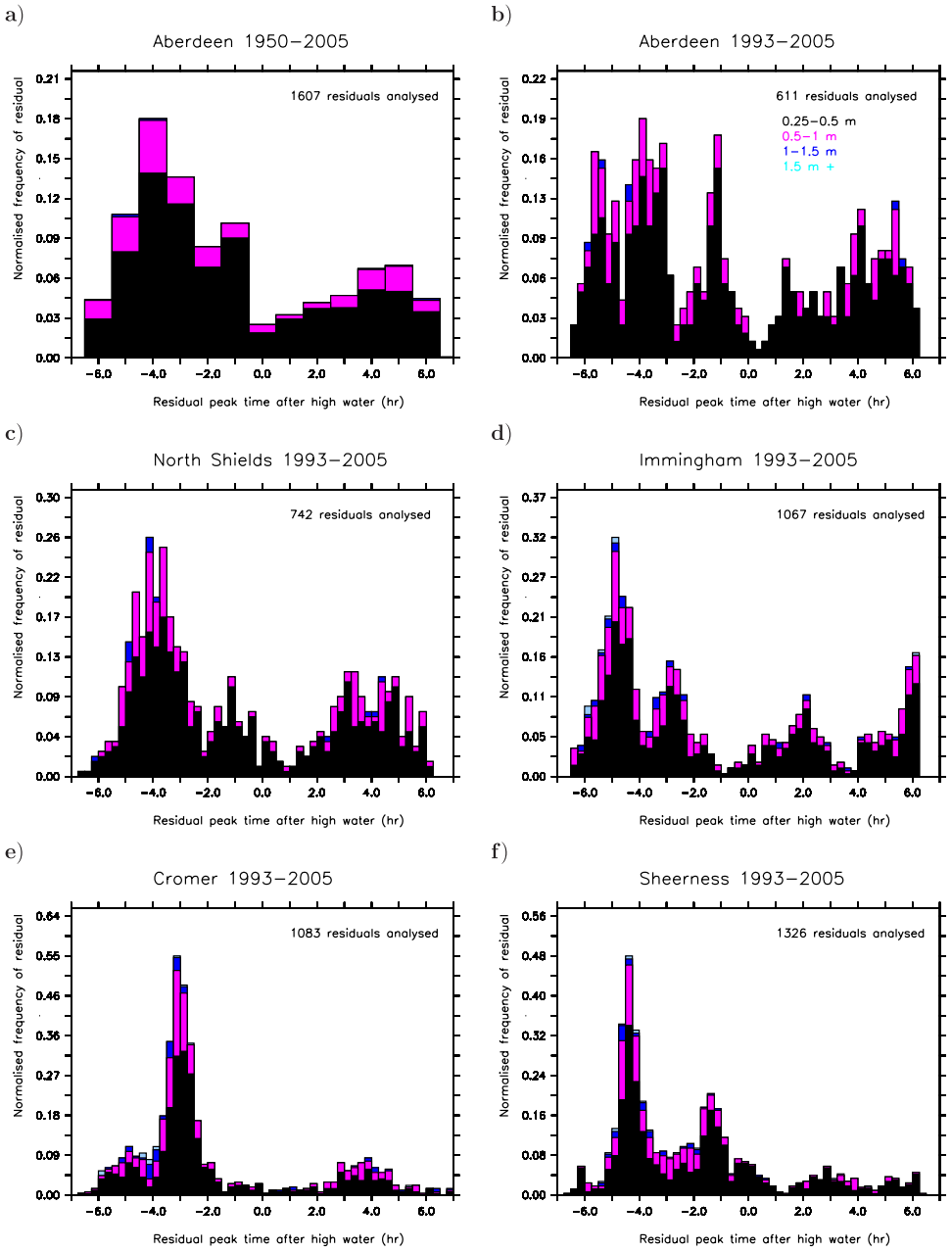

Figure 2. Normalized frequency of residual (greater than 25 cm) occurrence with respect to observed high water.

complex distribution but shows a definite additional peak 1 hour before high water (HW-1), which seems to coincide with a similar peak at North Shields (HW-1.5), Immingham (HW-2.5) and Sheerness (HW-1.5). The graphs also show that larger residuals are not encountered an hour on either side of high water. This is obviously of great practical interest for flood risk management, as is the mode found 1.5 hours prior to high water at Sheerness.

[9] Figure 3 shows the normalized frequency of negative residual events, with respect to the time of the nearest high water, for the five sites. For these events, more symmetry is displayed at Aberdeen. The multimodal pattern is again evident with a more complicated distribution at Sheerness and Immingham than for the positive residuals. Both of these sites are in shallow estuaries, and it is likely that the increased complexity results from the distortion of the higher harmonics of the tidal curves there because of shallower water. Furthermore, there are generally fewer events exceeding the selection threshold, which reflects the fact that high-pressure systems are less common than atmospheric depressions.

[10] The features apparent in Figures 2 and 3 result from tide-surge interaction. Since the passage of weather systems is independent of the tide, if the sea level was simply a linear superposition of tide and surge, then the peak residual could occur at any time with respect to high water (and the distributions would therefore be random). The important physics of this interaction can be explained easily. Assume

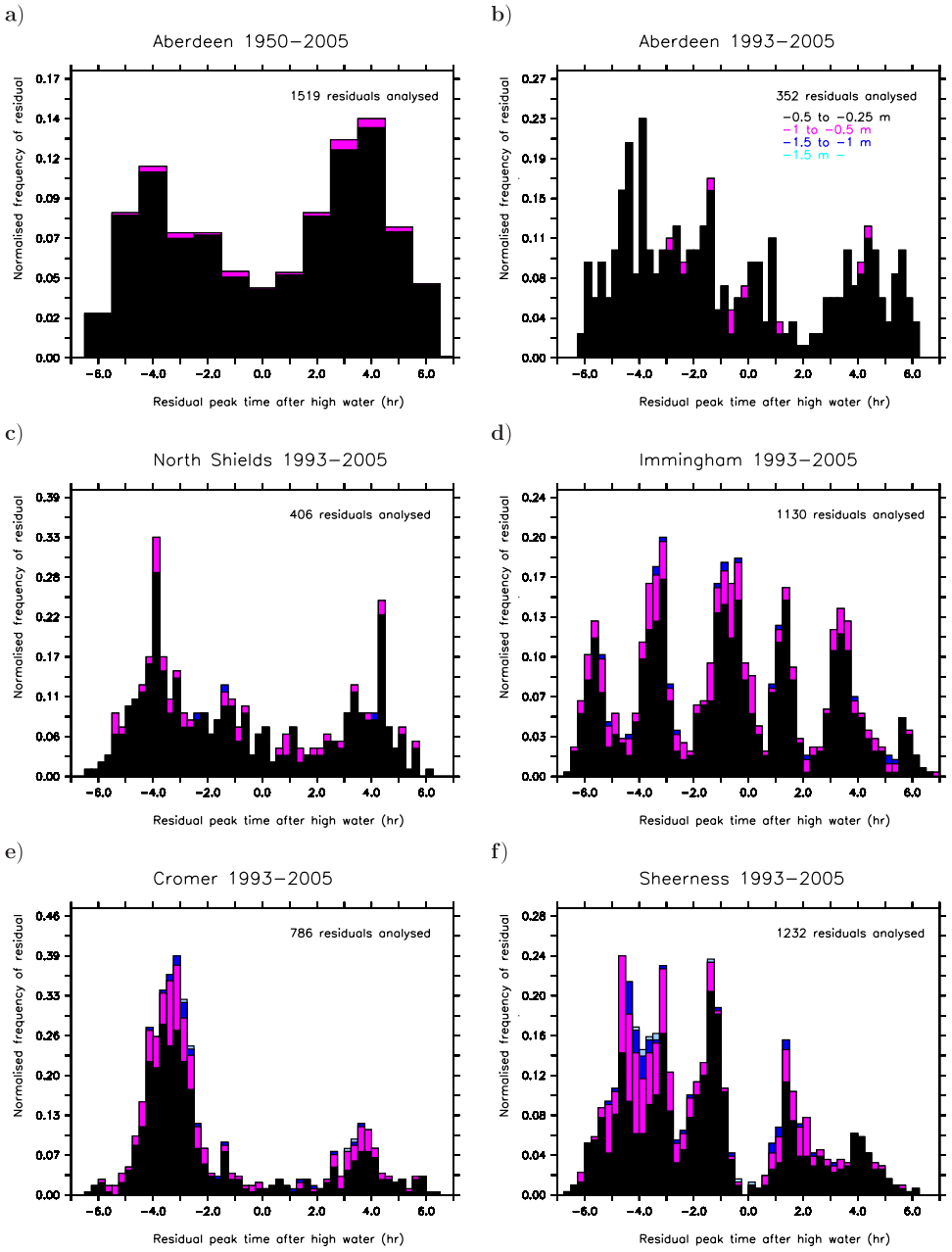

Figure 3. Normalized frequency of residual (less than −25 cm) occurrence with respect to observed high water.

that the dotted line in Figure 4 represents tidal predictions from the harmonic method and that the solid line depicts the actual sea level observations. In this instance, one can think of the tide as arriving sooner than predicted (due to meteorological effects, for example) although there is clearly no change to the amplitude of the sea level curve. If "surge" is defined as the observations minus the predictions (as is the case in most operational monitoring systems), then the dashed line is obtained, which has the same periodicity as the tide and a maximum on the rising tide.

[11] In this idealized example, elevation has not been increased by any surge-generating mechanism; a residual is obtained through the change of phase alone. This has previously been noted in a qualitative sense by *Rossiter* [1961], and also by *McInnes and Hubbert* [2003] for sea level residuals in Bass Strait, Australia. It is straightforward to develop a formal explanation for the effect. It can be shown (see Appendix A) that if the solid line in Figure 4 (observations) is $O = A\cos(\omega t)$ and the dotted line (tidal predictions) is $T = A\cos(\omega t - \varphi)$ where φ is a small (but nonzero) phase shift, then the residual curve, R, is given by:

$$R = B\cos(\omega t + \theta) \tag{1}$$

where

$$B = A(2 - 2\cos\varphi)^{1/2} \tag{2}$$

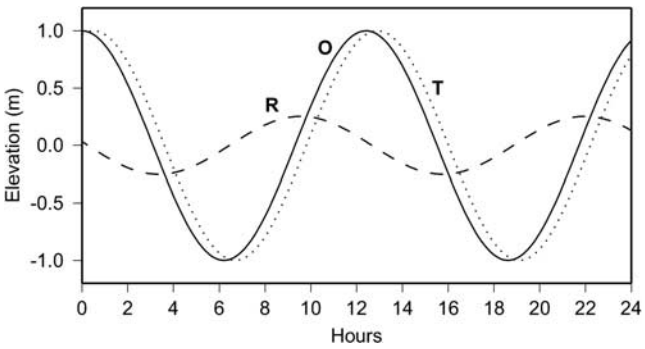

Figure 4. Schematic diagram of a sinusoid whose phase is altered but whose frequency and amplitude remain unaltered. The solid line (O) represents observations, the dotted line represents tidal predictions (T) and the dashed line represents the residual obtained via subtraction (R).

and

$$\theta = \tan^{-1}\left[\sin\varphi/(1-\cos\varphi)\right] \quad (3)$$

[12] For the situation shown in Figure 4 where the observations lead the predictions, Appendix A shows that, for small angles of φ, a good approximation to the behavior of the residual is that it peaks (in cyclic terms) 90° before the maximum in the observations, i.e., halfway up the rising tide. Conversely, if the observation curve lags the predictions then the residual peak will occur on the falling tide. This very simple model gives a first order explanation of the statistical properties of the tide-surge interaction. One expects a clustering on the rising tide, as seen in Figure 2, and a corresponding clustering on the falling tide on those occasions where sea level measurements lag the harmonic predictions. The implied phase changes are easily explained since both tides and surges (to first order) are shallow water waves, with phase speeds of $(gh)^{1/2}$ where h is the water depth and g is the acceleration due to the Earth's gravity. As noted by *Wolf* [1981], reduced water depth will result in a reduced phase speed both directly and because of the effects of bottom friction (which is inversely proportional to depth). A positive surge will increase the phase speed of both tide and surge as they travel along the coast.

[13] While phase shift is clearly important, the modes seen in Figures 2 and 3 indicate that additional mechanisms must be considered. It is necessary to explain the asymmetry of the distributions and the physical drivers that cause the main peak to be typically 4–5 hours before high water. It does not suffice to extend the simple model shown in Figure 4 and allow the tide to be amplified by a small factor as well as to be phase-shifted (not that this has any physical basis). It is easily shown (see Appendix A) that the inclusion of an amplification factor greater than unity causes the peak of the residual wave to move closer to high water. To obtain peak residuals that precede high water by more than 4 hours, as seen at several ports in Figure 2, we must combine the genuine rise in sea level brought about by meteorological effects with the impact of that surge on the dominant tidal signal. With regard to the asymmetry in Figure 2, only on the rising tide can a genuine surge constructively combine with the artifact due to the phase alteration (because greater water depth advances the time of high water). Of course, delayed high waters (due to negative surges) will also cause a phase-shifted residual on the falling tide but these are of less practical significance; now, when the effects of surge and phase shift are combined, they are less likely to exceed a given threshold, hence they are less frequent in the histograms.

3. Time Series at Sheerness for 99th Percentile Events

[14] Here we examine the observed sea level signal at Sheerness and the calculated residual, for the top 1% of residual events derived from the total set (1965–2005). Restricting the analysis to the largest residuals makes the task of interpreting their time series tractable, yet still provides 55 examples. It is also these events (corresponding to residuals that exceed 1.4 m) that are of practical significance for flood risk, particularly at this location, which is an indicator gauge for the operation of the Thames Barrier. The complete list is given in Appendix B, and the distribution of the time of maximum residual with respect to high water is shown in Figure 5. As the figure shows, the main cluster of 99th percentile residuals is found at 4 hours prior to high water, the same as for the total data set (Figure 2f). Residual peaks on the falling tide (HW+4) are also present in Figure 5 but there is no longer a subsidiary peak 1.5 hours before high water as there is in Figure 2f.

[15] It was possible to divide the time series into four distinct types, which are described and enumerated in Table 2. A minority displayed a combination of these characteristics, but 54 of the 55 events could be categorized unambiguously. Two-thirds were associated with a clear phase shift in the turning points of the observations with respect to the predicted tide; in the vast majority of these cases, the observations led the predictions and the maximum residual was found 4 hours before high water. In three cases, the observations lagged the predictions and then the maximum residual was observed 3–4 hours after

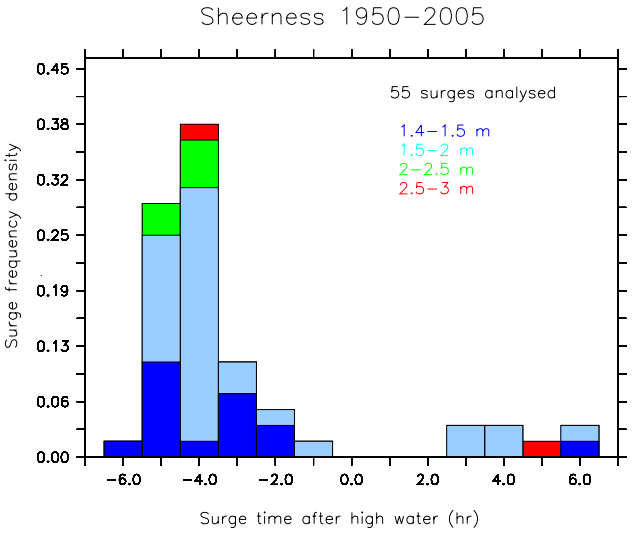

Figure 5. Frequency of time of maximum with respect to observed high water for the largest 1% of positive residuals at Sheerness.

Table 2. Classification of the Largest 1% of Residuals at Sheerness

Type	Characteristics	Number of occurrences
Phase altered	Distinct phase alteration to either HW or LW with respect to tidal predictions.	36
High water	No significant phase alteration. Residual is larger at HW than either adjacent LW.	3
Low water	No significant phase alteration. Residual is only significant at LW.	3
Long duration	Residual is significant for two or more HW and there is no significant phase alteration throughout. There is a dip in the residual at one or more HW.	12

high water. This lends credibility to the model put forward previously and reinforces the importance of phase shift as a key physical mechanism.

[16] Figure 6 shows an example of each type listed in Table 2, where the event chosen was that with the largest residual. With the exception of the three high water surges (Figure 6b), a feature common to all the other time series is that the residual is significantly greater at low water than at high water. This tidally modulated surge production is the other significant physical driver of the residual behavior. *Pugh* [1987] shows how one can obtain an idealized expression for the sea surface slope ($\partial\eta/\partial x$) that is in equilibrium with a constant wind field:

$$\partial\eta/\partial x = C\ W^2/H \tag{4}$$

where W is the wind speed in the x direction, H is the total water depth and C is a constant that combines the effects of gravity, density and an empirical drag coefficient. Of course, the wind field is rarely constant and such equilibrium is unlikely, but nevertheless, the expression makes the fundamental point that wind stress is more effective at raising the sea surface in shallow water. During a typical midlatitude depression, strong winds blow for 24 hours or more, and thus span more than one tidal cycle. One would expect any surge generated by wind stress to be larger at low water than at high water and this is evident in most of the events analyzed here.

[17] Inequality in surge generation does not necessarily imply that it is a local effect; as previously noted, surges may travel at roughly the same speed as the tidal wave. An enhanced surge could therefore be generated at low water elsewhere and travel in phase with the tidal trough. Surge generated in this way may well be enhanced in shallow water as suggested by *Proudman* [1955, 1957]. The characteristic dip in the residual near high water in Figure 6d reinforces the importance of tidally modulated surge production, and is typical of the long duration class. This temporary reduction in surge was thankfully evident in records of the North Sea floods of 31 January and 1 February 1953. In the next section, we use numerical models to show the influence of the tide on the generated surge.

4. Numerical Modeling

[18] Five of the surge events from Table B1 were simulated using a 12-km horizontal resolution, depth-averaged numerical model. The model (POL CS3) is used for operational surge forecasting in the UK and is described in detail by *Flather* [2000]. It is forced by surface pressure and 10-m wind fields supplied hourly by the UK Meteorological Office mesoscale model at a similar spatial

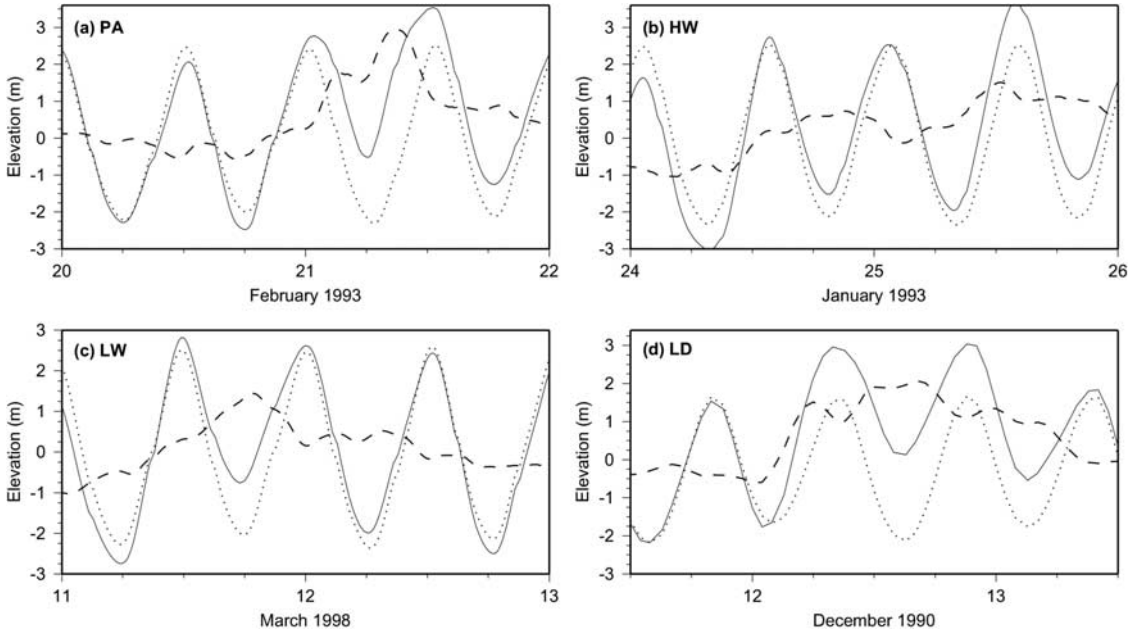

Figure 6. The largest for each type of residual event (see Table 2) at Sheerness. (a) Phase altered, (b) High water, (c) Low water, (d) Long duration. In all cases, the solid line represents observed sea level, the dotted line represents tidal predictions and the dashed line represents the calculated residual. The dates on the x axis denote 00Z on that day.

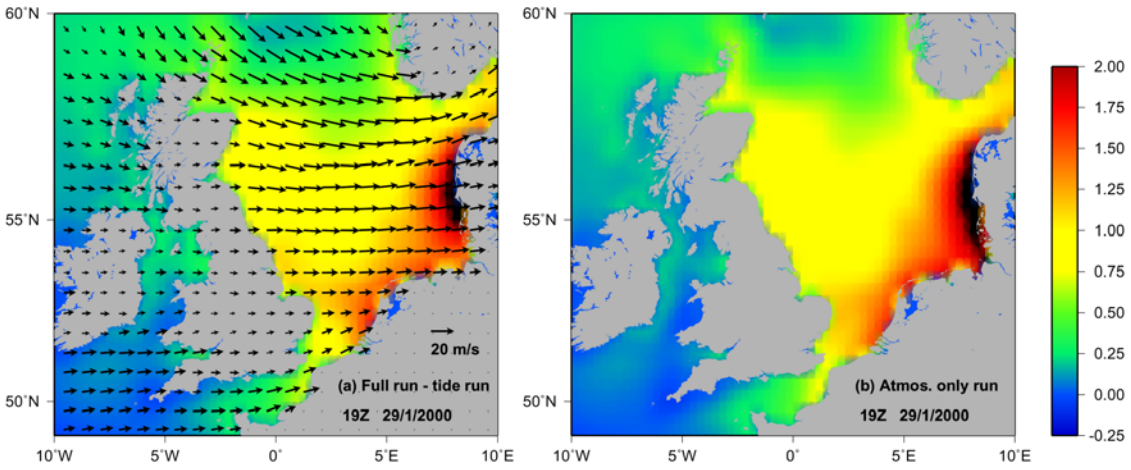

Figure 7. Modeled surge (m) at 19Z on 29 January 2000. (a) Residual calculated from fully forced run minus tidal run, (b) model run with atmospheric forcing only.

resolution. The tidal input to CS3 consists of the largest 26 constituents. The events modeled were chosen because the calculated model residuals agreed well with those calculated from the tide gauge data at the five sites. This gave a measure of confidence in the atmospheric forcing. The results presented are for the 29–30 January 2000, but are representative of all runs and illustrate the key conclusions drawn from the modeling.

[19] For each event, the tidal model was run with, and then without, atmospheric forcing in order to calculate a residual. The model tide was fully spun-up prior to each run. Runs were also performed with meteorological forcing only (no tide). The latter gives some insight into the effect of the tide on the surge generation and propagation. Figure 7a shows the calculated residual (full run minus tide only run) at 19Z on 29 January 2000, where the surge exceeds 2 m along parts of the Danish coast. Superimposed are the wind vectors, which illustrate the strong westerly winds that were present over the entire North Sea. The picture obtained when the model was run with atmospheric forcing only (Figure 7b) is qualitatively very similar. The pattern of the surge at the basin scale is dominated by the meteorological forcing and is insensitive to the state of the tide. This is not surprising since central parts of the North Sea are typically 50-m deep and tidal range is less than 2 m everywhere except along the east coast of the UK.

[20] Some differences between the plots can be discerned on close examination but the detailed differences are best visualized when the fields used to plot Figure 7 are subtracted from one another. The sequence shown in Figure 8 is the difference between the surge produced by meteorological forcing only and that obtained by subtraction of the tidal run from the fully forced run, over a full tidal cycle. The plots are annotated with the state of the tide at Sheerness. For the subsequent discussion, low water at Sheerness corresponds to high water at Cromer and to low water at Aberdeen; warm colors indicate that more surge is generated in the meteorology-only run than in the tidal run, whereas blue shading implies that more surge is produced in the tidal run. In Figure 8a, sea level is elevated to an additional 0.5 m between Immingham and Cromer in the meteorology-only run. This is consistent with equation (4) and reduced surge production because of the fact that it is high water there in the tidal run. At the same time, surge is enhanced at Aberdeen in the tidal run (because it is low water there). The pattern moves, in the same sense as the tide itself, toward high water at Sheerness (Figure 8c) where there is then a diminished surge in the tidal run. Contemporaneously, in the tidal run, there is a reduction in surge at Aberdeen. By the next low water at Sheerness (Figure 8e), the pattern has reverted to that of Figure 8a, but this time showing a distinct increase in surge at Sheerness in the tidal run. The results in Figure 8 demonstrate the tidally modulated surge production. The magnitude of the modulation will obviously vary by event and by location, and will have a complicated dependency on wind speed and direction, the spring-neap cycle and the timing of the weather system with respect to the state of the tide.

[21] This modulation is also apparent in the model residual time series at the tide gauge sites. The left-hand panels in Figure 9 are from the same model run as in Figure 8, and the right-hand panels show a second event from 30 January 2003. For both dates, the modulation of the surge is evident around high water where the difference between the residual (solid line) and the meteorology-only run (dashed line) is of the order 0.3–0.5 m. The surge is prevented from peaking at high water even if the strongest meteorological forcing is at that time. It is interesting to note that when viewed over several tidal cycles, the calculated residual and the surge are broadly similar; a lowpass filter with appropriate parameters would render the two indistinguishable. This implies that the response of the North Sea to the larger scale development of meteorological forcing is not affected by local tidal response, although the local detail is obviously necessary for accurate forecasting.

[22] The open circles in Figure 9 depict additional model runs where the wind-forcing was artificially removed at a certain time. These experiments were designed to evaluate the significance of local reinforcement of the surge compared with that propagating as a wave (sometimes referred to as external surge). In Figure 9a, the open circles show results from a run where the wind field was smoothly

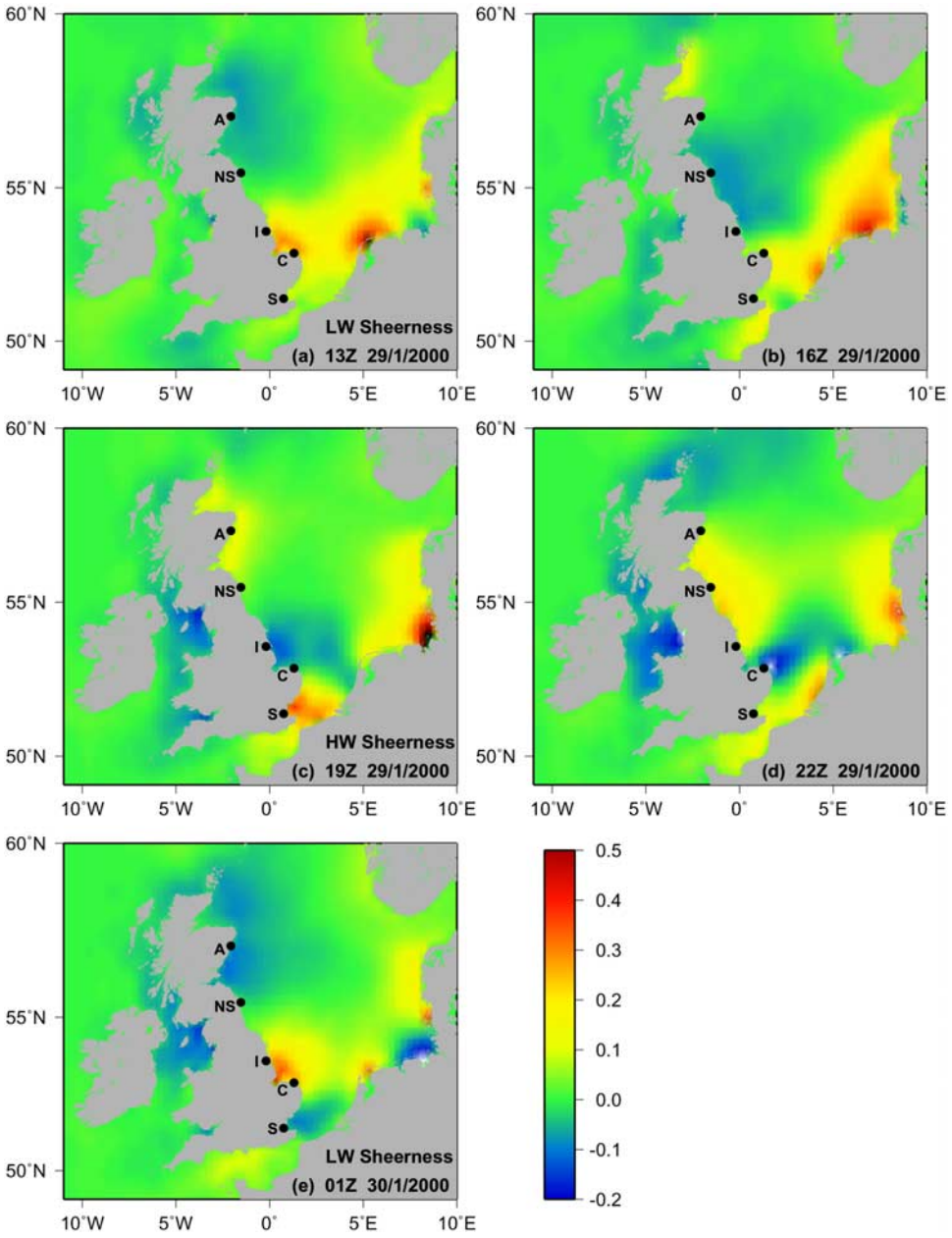

Figure 8. The local modulation of the surge (m) caused by tidal effects, calculated by subtracting the residual (itself a subtraction of tide from fully forced run) from an atmosphere-only forced run. The tide gauge sites from Figure 1 are marked with their initials, and the state of the tide at Sheerness is given.

reduced to zero between 22Z and 24Z on 29 January 2000, by which time the surge was well developed at Cromer. The surge decays more rapidly than the meteorology-only run (dashed line) but peaks at the same time. At Sheerness (Figure 9b), the difference between the open circles and the dashed line suggests that local wind enhancement serves to both increase the size of the surge and cause the peak to be delayed. The difference at 05Z on 30 January 2000 is approximately 0.5 m. This amounts to 25%–30% of the surge being locally generated and is consistent with the findings of *Prandle* [1975] who performed a model simulation of the disastrous 1953 surge. In the second relaxation run, the wind was removed between 11Z and 13Z on 30 January 2003 which still allowed the surge to develop fully at Immingham (see Figure 9c). There are inertial oscillations of approximately 8 hours period in all model runs at this time. It is evident from Figure 9d that the surge at Sheerness is now reduced by as much as 1 m. The implication is that although the surge was fully developed at Immingham, significant further development is required to create the surge at Sheerness.

5. A Simple Model to Explain Residual Clustering

[23] The numerical model results show the modulation of surge production as a result of water depth. Although the nonlinearity of the tide-surge system means that separable

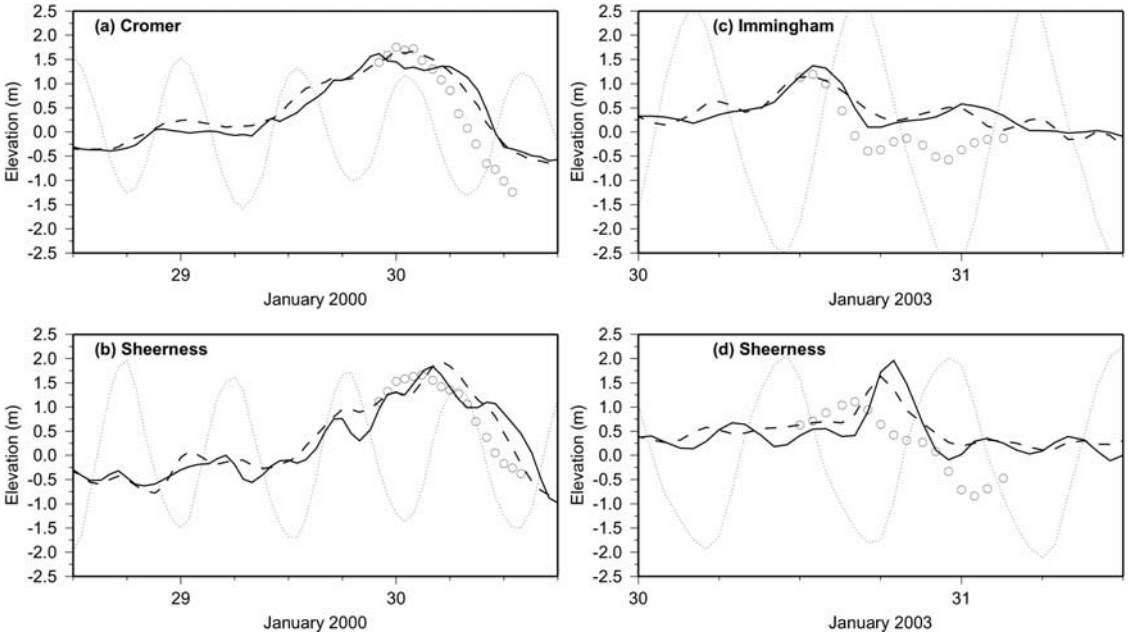

Figure 9. Time series of the 29 January 2000 surge at (a) Cromer and (b) Sheerness, and 30 January 2003 surge at (c) Immingham and (d) Sheerness. The solid line is the residual calculated by subtracting the tidal run from the full run; the dashed line is the surge from the atmosphere only run; the faint dotted line shows the tidal elevation. Open circles are from runs where winds were relaxed gradually to zero as specified in the text. The dates on the *x* axis denote 00Z on that day.

solutions of the full dynamical equations are not mathematically feasible, there are two distinct physical mechanisms that dominate in very shallow water: these are the phase shift of the tidal signal due to the surge, and the modulation of surge production due to the tide. These are now combined in the simplest possible model that explains the histogram distributions seen in Figure 2 by assuming a surge with local semidiurnal modulation that causes the maximum to occur at low water, but which is otherwise constant. It is shown in Appendix C that the peak in the residual with respect to the time of predicted high water is given by:

$$(\theta + \varphi) = \tan^{-1}\left[\sin\varphi/(1 - \cos\varphi + k)\right] - \pi \qquad (5)$$

where φ is the tidal phase alteration as before, and k is the ratio of the local surge modulation to the tidal amplitude. Solution curves for various values of φ are shown in Figure 10 where the residual peak phase has been converted to time assuming a 12.4-hour cycle. Figure 10 demonstrates how for small values of tidal phase shift only modest amounts of local surge modulation are required to cause the residual to peak at 4 or 5 hours before high water, as seen in Figure 2 for the modes of Sheerness and Immingham, respectively. Increasing the amount of local modulation moves the peak residual toward low water, so the implication is that local effects are more significant at Immingham than elsewhere. The local mechanism is less effective for larger values of tidal phase shift. Although there is a mathematical symmetry to the solutions, we have chosen to focus on those corresponding to positive phi because this represents the physical situation where a genuine positive surge increases sea level (hence increases the phase speed of a long wave) and therefore advances high water. In this instance, the effects of phase shift and surge are constructive, so this is the case of greatest practical significance. It is easy to show that, for negative values of tidal phase shift, a mirror image of Figure 10 is obtained, with the solutions falling between 3 hours after high water and low water.

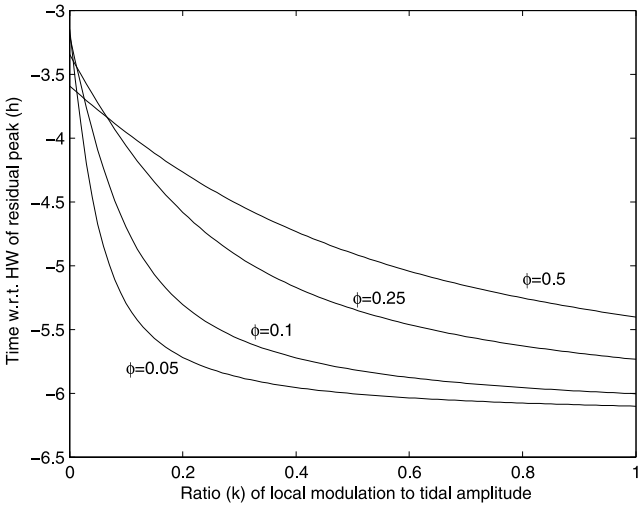

Figure 10. Curves showing the time of peak residual with respect to predicted high water for a variety of surge modulation/tidal amplitude ratios (k) when combined with different tidal phase shifts (φ, rads).

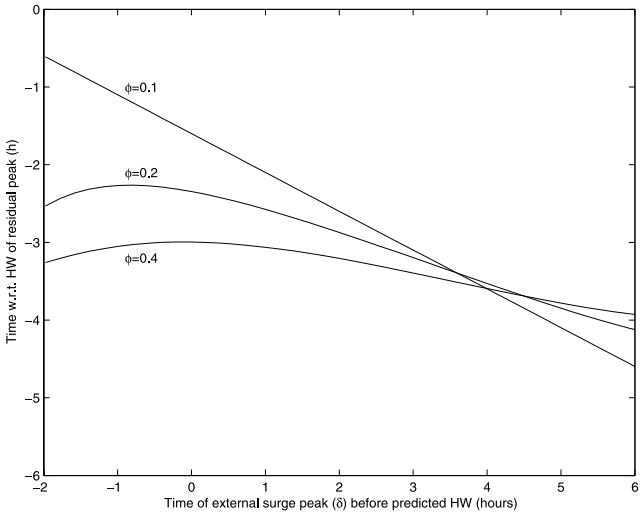

Figure 11. Curves showing the time of peak residual with respect to predicted high water for a variety of external surge arrival times (δ) combined with different tidal phase shifts (φ, rads). For this family of curves, the surge modulation/tidal amplitude ratio is $k = 0.1$.

[24] To permit, only local modulation is oversimplistic, since an external component of surge can account for a significant portion of the meteorological impact as seen in Figure 9. A final model is proposed that consists of a constant surge augmented by a semidiurnal modulation that can now take any phase lag with respect to the predicted high water. This phase (δ) will depend upon the distance over which an external surge has been reinforced, and also correctly reflects the fact that the onset of strong winds is independent of the tide. Appendix C shows that the peak in the residual with respect to predicted high water is now given by:

$$(\theta + \varphi) = \tan^{-1}\left[(\sin\varphi + k\sin\delta)/(1 - \cos\varphi - k\cos\delta)\right] - \pi \quad (6)$$

and when $\delta = \pi$ (local modulation), this equation is identical to equation (5).

[25] Tidal amplitudes along the east coast of the UK are in the range 1.5–2.5 m, depending on the state of the spring-neap cycle and the exact location. From Figure 9, it can be inferred that the surge modulation due to the tide is in the range 0.1–0.5 m. Therefore solutions to equation (6) are presented for two values of the surge modulation/tidal amplitude ratio: $k = 0.1$ and $k = 0.3$, with the larger ratio being consistent with large modulation during a neap tide. Figure 11 shows the expected timing (with respect to predicted high water) of the peak-calculated residual for tidal phase shifts of $\varphi = 0.1$, 0.2 and 0.4 (corresponding to 10, 20 and 40 min), for external surge peaks arriving between low water and 2 hours after high water.

[26] Figure 11 shows that, for physically realistic arrival times of any external surge component, the residual peak will always avoid high water (and low water) for any finite tidal phase shift. For small positive phase shifts, it is possible to obtain a residual peak at high water only when the external surge peaks around 3 hours after high water (not shown); however, in this case, the effects of genuine surge and the phase shift mechanism are destructive, so the residual is almost zero. For larger tidal phase shifts, this does not occur since $\sin\varphi > k \sin\delta$ in the numerator of equation (6), and as indicated by the convexity of the solutions for $\varphi = 0.2$ and $\varphi = 0.4$ in Figure 11.

[27] The effect of a larger ratio, k, can be seen in Figure 12. It is clear from Figures 11 and 12 that smaller values of k restrict the range of times at which the residual peak can occur. When surges are proportionally smaller, the residual has a greater tendency to peak between 2 and 4 hours before high water for any phase of external surge. An increase in the tidal range decreases the ratio, k, and makes it less possible for the residual peak to coincide with high water. This is of great importance for coastal flooding since the results imply that, for large tides (those of concern to engineers and planners), the peak residual is far more likely to follow the solutions shown in Figure 11 and will therefore be found further away from high water.

6. Discussion

[28] The details of the distributions in Figure 2 have not been previously shown and are possible because of the improved data availability and its temporal resolution. The results confirm the earlier work of *Rossiter* [1961] and *Prandle and Wolf* [1978], who put forward explanations for the predominance of residual maxima on the rising tide. However, the higher temporal resolution of our sea level observations shows precisely how the modes of residual maxima are related to predicted high water at each of the tide gauge locations. We also reveal an additional mode that occurs approximately 1–2 hours before high water at several of the sites. With regard to the primary mode, our histograms from 1993 to 2005 show no significant differences from the diagrams of *Prandle and Wolf* [1978], which implies that there is no decadal change to the pattern of tide-surge interaction. Since tide-surge interaction is

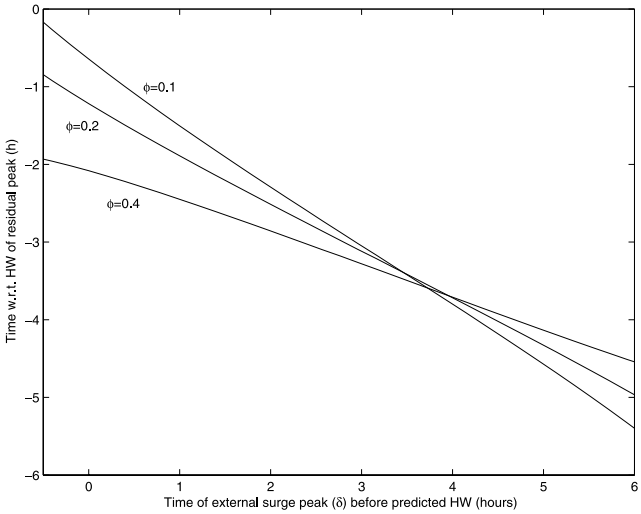

Figure 12. Curves showing the time of peak residual with respect to predicted high water for a variety of external surge arrival times (δ) combined with different tidal phase shifts (φ, rads). For this family of curves, the surge modulation/tidal amplitude ratio is $k = 0.3$.

sensitive to small changes in tidal phase, mean sea level rise could affect the frequency distribution of surges in specific locations. This in turn could impact the statistics of extremes used in the calculation of return periods. The clustering of residual maxima is not restricted to estuaries, but is also evident at coastal locations such as Aberdeen and North Shields; this contradicts *Pugh and Vassie* [1980] who state that there is little tide-surge interaction outside of estuaries.

[29] We have shown that many properties of a nontidal residual time series stem from the choice of definition (i.e., that surge is the observed sea level minus the tidal predictions). Of course, in an arithmetic sense, this is perfectly correct but it can be misleading if one wishes to quantify sea level change due to genuine meteorological drivers. Thus residuals calculated from tide gauge records are often largely an artifact of the subtraction process since they also contain all errors of timing. A residual can arise from phase shift alone in the absence of any meteorological enhancement, as we show in Figure 4. The existence of semidiurnal oscillations in the residual signal has long been recognized, as has the fact that they can be caused by phase alteration of the tidal signal [*Rossiter*, 1961; *Heaps*, 1983; *McInnes and Hubbert*, 2003; *Bernier and Thompson*, 2006]. Equations (1)–(3) give further insight into the phenomenon of tide-surge interaction and the reason for residual maxima to preferentially occur on a rising tide. This raises the issue that subtraction is not necessarily the best way to extract genuine meteorological effects. Indeed, in other disciplines (for example, signal processing), the subtraction of two very similar signals is known to magnify noise. When a residual is obtained purely as a result of phase shift, then that shift can be estimated from the amplitude of the oscillating residual as we show in equation (A3); thus it may be possible to correct for the phase shift, although the complexity of the oceanographic situation would often prevent this. Previous empirical and theoretical analyses [*Keers*, 1968; *Cartwright*, 1968; *Prandle and Wolf*, 1978] have all suggested that the tide-surge interaction increases in direct proportion to both surge height and tidal range. This is to be expected since equation (2) shows how, to first order, any such interaction scales on the amplitude of the predicted tide.

[30] Our numerical model results indicate that surge generation is modulated by the state of the tide. Simply put, the modulation of surge production represents the effect of the tide on the surge, while a phase shift of the tidal signal represents the effect of the surge on the tide. The occurrence of residual maxima 4 hours prior to high water at Sheerness, and 5 hours before high water at Immingham, can be attributed to relatively small amounts of local surge modulation. There is an implication that Cromer experiences little surge modulation, since its peak residual occurrence is close to 3 hours before high water. The fact that surge generation is less affected by the tidal state at Cromer may be because of the relatively small tidal range in the surrounding area (being close to an amphidrome), and also that it is on a part of the coastline exposed to the surge-producing northerly winds typical of North Sea surges.

[31] The physical model does not explain the grouping of residual peaks found 1–2 hours in advance of high water at the majority of sites. One hypothesis is that these modes represent phase differences for higher tidal harmonics. It is well understood that nonlinear terms in the equations of motion can generate the quarter diurnal and higher order overtides (for example, the M_4 and M_6 constituents). If these constituents differed between observations and predictions, then the residual time series would exhibit peaks at approximately 1.5 and 4.5 hours before high water. The latter group would be indistinguishable from the primary group in Figure 2. Furthermore, since the quarter diurnal constituents are fairly small in amplitude, then the residual amplitude would also be small. This is consistent with the disappearance of this mode in Figure 5. The degree to which tide-surge interaction during extended periods of meteorological forcing can modify the generation of shallow water constituents is an interesting subject for future study.

[32] It is important to recognize that surges are not freely propagating Kelvin waves, but respond very strongly to the presence or absence of meteorological reinforcement; *McInnes and Hubbert* [2003] review the debate surrounding the dynamics of propagating, wind-forced coastally trapped waves on the south coast of Australia. Our results point to the existence of locally determined, temporal and spatial scales for surge development and decay. The model results using the relaxation of the meteorological forcing (Figure 9) demonstrate that a significant enhancement of the surge can occur between Immingham and Sheerness, and that the decay scales are of the order 3 hours or 100 km. These scales are likely to be highly dependent on location, topography and the level of equilibrium attained between the surface elevation and the meteorological forcing. For parts of a surge's life span, it may be that direct wind-forcing is more important than wave propagation, as is true of hurricanes [e.g., *Morey et al.*, 2006].

[33] Our results contain important conclusions of interest to flood risk managers and coastal engineers. Figure 2 shows that larger surges are only encountered around 3–5 hours before high water and never within an hour of high water. Our models suggest that for physically realistic arrival times of any external surge component, the residual peak will always avoid high water (and low water) for any finite tidal phase shift. The analysis of large, long duration surge events confirms that surge generation is reduced at high water. Furthermore, increasing tidal range appears to reduce the risk of residual peaks arriving near high water. It follows from this work that any risk analysis must recognize the dependence of tide and surge. This could affect guidance given for coastal management that is currently precautionary in the UK, considering the surge and tide as potentially coincident.

[34] The models proposed here are extremely simple and describe only some of the possible interactions between tide and surge since we make no attempt to couple the mechanisms hydrodynamically. Nevertheless, they provide plausible explanations of residual timing and hopefully provide an insight for further dynamical analysis. For practical forecasting purposes, the only thing that matters is an accurate prediction of the total water level at any time. Presently, the UK's operational coastal flood warning system [*Flather*, 2000] derives tides locally from harmonic predictions, and then adds a numerical model simulation

which incorporates both surge and tide-surge interaction. Other operational systems superpose an atmosphere-only forced surge onto a tidal model [e.g., *Bobanovic et al.*, 2005] but recognize the need to include the effects of tide-surge interaction. All of the foregoing provides a strong motivation to improve the performance of numerical models used in forecasting such that total modeled water levels are predicted with confidence. Calculation of ambiguous residuals then becomes unnecessary.

Appendix A

[35] Assume that a set of sea level observations are phase advanced by an amount, φ, with respect to the corresponding tidal predictions (here, the frequency, ω, refers to the total tide over a small number of cycles rather than any individual constituent) and that amplitude, A, remains unchanged. It is convenient for now to reference everything to the observations. Since we are manipulating harmonics of one frequency, complex exponential form is used below. When the residual, R, is calculated by subtracting the predictions from the observations then:

$$\begin{aligned} R &= A\cos(\omega t) - A\cos(\omega t - \varphi) \\ &= \Re[Ae^{i\omega t}(1 - e^{-i\varphi})] \\ &= \Re[Ae^{i\omega t}(1 - \cos\varphi + i\sin\varphi)] \\ &= B\cos(\omega t + \theta) \end{aligned} \tag{A1}$$

where θ is given by:

$$\begin{aligned} \tan\theta &= \sin\varphi/(1 - \cos\varphi) \\ &= (\varphi - \varphi^3/3! + \varphi^5/5! - \ldots.)/(1 - 1 + \varphi^2/2! - \varphi^4/4! + \ldots) \\ &\approx 2/\varphi \text{ as } \varphi \text{ becomes small} \\ &\quad \underline{\rightarrow \infty \text{ as } \varphi \rightarrow 0} \end{aligned} \tag{A2}$$

As the phase shift between observations and predictions, φ, tends to zero the phase advance of the residual, $\theta = 90°$. In cyclic terms, the peak of the residual wave leads the observed high water by 90°.

[36] The magnitude of the residual is obtained by Pythagorean Theorem:

$$\mathrm{B} = \mathrm{A}(2 - 2\cos\varphi)^{1/2} = \underline{\mathrm{A}\varphi \text{ for small values of } \varphi} \tag{A3}$$

The residual amplitude is seen to be scaled by the tidal amplitude and the phase shift.

[37] The arithmetic is similar if we now allow the observations to be amplified by a small factor, α, in addition to being phase-shifted as before. We include this for completeness, although it is physically unlikely since amplification at high water is precluded by the surge physics as discussed. Now:

$$\mathrm{R} = \Re\left[Ae^{i\omega t}(\alpha - \cos\varphi + i\sin\varphi)\right]$$

and $\tan\theta = \sin\varphi/(\alpha - \cos\varphi)$.

[38] The denominator prevents the tangent of θ from approaching infinity, and therefore for any value of α greater than unity, the residual wave peak moves toward the peak of the observations.

Appendix B

[39] Table B1.

Table B1. The Largest 1% of Residuals at Sheerness (Those Greater Than 1.4 m) From the Complete Data Set (1965–2005)[a]

Maximum height of residual, m	Time of peak w.r.t. high water, h	Time and date when 1.4 m threshold was first exceeded	Duration above threshold, (hr)	Type (see Table 2)
1.648	−4.000	1965/02/14, 06:00:00	3.000	LD
1.557	−1.000	1965/12/10, 12:00:00	1.000	HW
1.451	−3.000	1967/03/18, 13:00:00	2.000	PA
1.474	−5.000	1967/04/05, 16:00:00	2.000	PA
1.771	−4.000	1967/04/06, 07:00:00	2.000	PA
1.595	−5.000	1968/01/11, 04:00:00	1.000	LW
2.212	−5.000	1968/03/06, 08:00:00	16.000	LD
2.254	−4.000	1969/09/29, 09:00:00	4.000	PA
1.597	−4.000	1970/04/29, 13:00:00	3.000	PA
1.847	−4.000	1971/11/21, 21:00:00	4.000	PA
1.829	−4.000	1973/04/02, 19:00:00	4.000	PA
1.491	−3.000	1973/11/19, 17:00:00	1.000	LD
1.491	6.000	1973/12/14, 22:00:00	1.000	LD
1.872	−5.000	1974/12/13, 06:00:00	3.000	LW
1.477	−4.000	1981/01/01, 17:00:00	1.000	PA
1.896	−5.000	1981/11/24, 18:00:00	4.000	PA
1.646	−4.000	1982/11/13, 06:00:00	3.000	PA
1.671	−4.000	1982/11/16, 20:00:00	3.000	PA
1.577	−4.000	1983/01/18, 10:00:00	4.000	PA
2.163	−4.000	1983/02/01, 22:00:00	5.000	PA
1.765	−4.000	1984/01/04, 08:00:00	3.000	PA
1.656	−4.000	1985/01/06, 19:00:00	3.000	PA
1.465	−3.000	1985/04/28, 02:00:00	2.000	LD
1.696	4.000	1985/11/06, 08:00:00	7.000	LD
1.896	6.000	1985/12/26, 17:00:00	4.000	LD
1.512	−4.000	1986/01/24, 08:00:00	2.000	PA
1.469	−3.000	1987/03/28, 20:00:00	2.000	PA
1.493	−6.000	1988/02/29, 02:00:00	17.000	LD
2.521	5.000	1989/02/14, 07:00:00	9.000	–
1.424	−5.000	1990/09/21, 09:00:00	1.000	PA
1.523	−4.000	1990/10/07, 09:00:00	2.000	PA
2.079	−5.000	1990/12/12, 06:00:00	14.000	LD
1.437	−4.500	1993/01/18, 03:45:00	1.000	PA
1.510	−1.750	1993/01/25, 11:45:00	1.750	HW
1.675	3.250	1993/02/19, 13:30:00	2.750	PA
2.941	−4.000	1993/02/21, 02:30:00	9.500	PA
1.607	−4.750	1993/11/14, 19:15:00	2.250	PA
1.467	−2.000	1993/12/20, 02:15:00	1.000	HW
1.673	−2.750	1994/01/28, 08:45:00	3.000	PA
1.543	−4.250	1995/01/01, 19:30:00	13.250	LD
1.707	3.500	1995/01/10, 08:00:00	4.500	PA
1.829	−4.500	1996/02/19, 07:15:00	3.750	PA
1.414	−2.000	1996/10/29, 12:00:00	0.500	PA
1.441	−5.000	1998/03/11, 18:30:00	1.000	LW
2.032	−4.000	1999/02/04, 21:45:00	16.000	LD
1.488	−4.500	1999/02/17, 08:30:00	1.250	LD
1.626	−4.250	1999/11/06, 18:15:00	3.000	PA
1.879	−3.500	2000/01/30, 01:15:00	5.000	PA
1.463	−4.750	2002/02/21, 00:45:00	1.500	PA
1.529	−2.500	2002/02/22, 16:15:00	2.000	PA
1.701	−5.250	2002/10/27, 21:30:00	2.750	PA
1.740	−5.000	2003/01/30, 17:15:00	2.500	PA
1.586	−3.750	2003/12/14, 23:15:00	2.750	PA
1.523	4.500	2003/12/21, 13:00:00	3.000	PA
1.882	−4.750	2004/02/08, 20:00:00	2.750	PA

[a]Key to residual type: PA, phase altered; LD, long duration; HW, high water; LW, low water.

Appendix C

[40] We retain the simple model of Appendix A and now add a first order approximation to the surge modulation. For simplicity, the surge is represented as a constant part, S, with a local semidiurnal modulation of amplitude, L, that peaks at low water. The tidal amplitude is A and the tidal phase shift is φ as previously mentioned. Now let $L = kA$, where k is the ratio of the surge modulation to the tidal amplitude. The residual, R_p, is given by the following expression where everything is now referred to predicted high water:

$$\begin{aligned} R_p &= \text{phase altered tide} - \text{predicted tide} + \text{constant surge} \\ &\quad + \text{local surge modulation} \\ &= A\cos(\omega t + \varphi) - A\cos(\omega t) + S + kA\cos(\omega t + \pi) \\ &= \Re\left[Ae^{i(\omega t+\varphi)} - Ae^{i\omega t} + kAe^{i(\omega t+\pi)}\right] + S \\ &= \Re\left[Ae^{i\omega t}\left(e^{i\varphi} - 1 + ke^{i\pi}\right)\right] + S \end{aligned} \tag{C1}$$

We differentiate w.r.t. time in order to locate the turning points of R_p.

$$\begin{aligned} R_p' &= \Re[i\omega Ae^{i\omega t}(e^{i\varphi} - 1 + ke^{i\pi})] = 0 \\ &=> \Re[(i\cos\omega t - \sin\omega t)(\cos\varphi + i\sin\varphi - 1 - k)] = 0 \end{aligned} \tag{C2}$$

and the following solution is obtained:

$$\omega t = \tan^{-1}\left[\sin\varphi/(1 - \cos\varphi + k)\right] - \pi \tag{C3}$$

where the subtraction of π ensures that the time angle ωt is consistent with the leading angle notation used in Appendix A. If φ is positive and tan θ is as given in equation (A3), then:

$$-(\theta + \varphi) = \theta - \pi \tag{C4}$$

When $k = 0$ in equation (C3) (i.e., there is no local modulation), then $-\omega t = (\theta + \varphi)$ and the turning point obtained agrees with the peak residual predicted earlier. For negative phase shifts ($\varphi < 0$), when the tidal curve is delayed, a consistent solution is obtained from:

$$\omega t = \tan^{-1}\left[\sin\varphi/(1 - \cos\varphi + k)\right] + \pi \tag{C5}$$

[41] Finally, this model is extended by permitting the surge modulation term to peak at any time, by replacing π in equation (C1) with a variable phase, δ. Setting the derivative of the residual to zero now gives:

$$\Re[(i\cos\omega t - \sin\omega t)(\cos\varphi + i\sin\varphi - 1 + k\cos\delta + ik\sin\delta)] = 0 \tag{C6}$$

and collecting terms together give the solution:

$$\omega t = \tan^{-1}\left[(\sin\varphi + k\sin\delta)/(1 - \cos\varphi - k\cos\delta)\right] \pm \pi \tag{C7}$$

In the absence of the tidal phase shift, the residual peak occurs at an angle δ before predicted high water; that is, it corresponds to the external surge arrival.

[42] **Acknowledgments.** The work described here was partly funded by the UK Environment Agency under the TE2100 (EP17) program, and by the Natural Environment Research Council (NERC). We are grateful to the British Oceanographic Data Centre (BODC) for supplying the tide gauge data. Some of the figures in this paper were generated using the Generic Mapping Tools [*Wessel and Smith*, 1998].

References

Bernier, N. B., and K. R. Thompson (2006), Predicting the frequency of storm surges and extreme sea levels in the northwest Atlantic, *J. Geophys. Res.*, *111*, C10009, doi:10.1029/2005JC003168.

Bobanovic, J., K. R. Thompson, S. Desjardins, and H. Ritchie (2005), Forecasting storm surges along the east coast of Canada and the northeastern US: the storm of 21 January 2000, *Atmos.-Ocean*, *44*(2), 151–161.

Cartwright, D. E. (1968), A unified analysis of tides and surges round north and east Britain, *Philos. Trans. R. Soc. Lond., A*, *263*, 1–55.

Doodson, A. T. (1929), Report on Thames floods, *Geopys. Mem. Lond.*, *47*, 1–26.

Flather, R. A. (2000), Existing operational oceanography, *Coast. Eng.*, *41*, 13–40.

Heaps, N. S. (1983), Storm surges 1967–1982, *Geophys. J. R. Astron. Soc.*, *74*, 331–376.

Keers, J. F. (1968), An empirical investigation of interaction between storm surge and astronomical tide on the east coast of Great Britain, *Dtsch. Hydrogr. Z.*, *21*, 118–125.

Lavery, S., and W. Donovan (2005), Flood risk management in the Thames estuary looking ahead 100 years, *Philos. Trans. R. Soc. Lond., A*, *363*, 1455–1474.

McInnes, K. L., and G. D. Hubbert (2003), A numerical modelling study of storm surges in Bass Strait, *Aust. Meteorol. Mag.*, *52*, 143–156.

McRobie, A., T. Spencer, and H. Gerritsen (2005), The Big Flood: North Sea storm surge, *Philos. Trans. R. Soc. Lond., A*, *363*, 1263–1270.

Morey, S. L., S. Baig, M. A. Bourassa, D. S. Dukhovskoy, and J. J. O'Brien (2006), Remote forcing contribution to storm-induced sea level rise during hurricane Dennis, *Geophys. Res. Lett.*, *33*, L19603, doi:10.1029/2006GL027021.

Prandle, D. (1975), Storm surges in the southern North Sea and River Thames, *Philos. Trans. R. Soc. Lond., A*, *344*, 509–539.

Prandle, D., and J. Wolf (1978), The interaction of surge and tide in the North Sea and River Thames, *Geophys. J. R. Astron. Soc.*, *55*, 203–216.

Proudman, J. (1955), The propagation of tide and surge in an estuary, *Proc. R. Soc. Lond.*, *A231*, 8–24.

Proudman, J. (1957), Oscillations of tide and surge in an estuary of finite length, *J. Fluid Mech.*, *2*, 371–382.

Pugh, D. T. (1987), *Tides, Surges and Mean Sea-Level: A Handbook For Engineers And Scientists*, 472 pp., John Wiley, Hoboken, N. J.

Pugh, D. T., and G. A. Maul (1999), Coastal sea level prediction for climate change, in *Coastal Ocean Prediction. Coastal and Estuarine Studies*, vol. 56, pp. 377–404, AGU, Washington D. C.

Pugh, D. T., and J. M. Vassie (1980), Applications of the joint probability method for extreme sea level computations, *Proc.-Inst. Civ. Eng.*, *69*, 959–975.

Rossiter, J. R. (1961), Interaction between tide and surge in the Thames, *Geophys. J. R. Astron. Soc.*, *6*, 29–53.

Tawn, J. A., and J. M. Vassie (1989), Extreme sea levels: The joint probabilities method revisited and revised, *Proc.-Inst. Civ. Eng.*, *87*, 429–442.

Wessel, P., and W. H. F. Smith (1998), New improved version of Generic Mapping Tools released, *Eos Trans. AGU*, *79*, 579.

Wolf, J. (1981), Surge-tide interaction in the North Sea and River Thames, in *Floods due to High Winds and Tides*, edited by D. H. Peregrine, pp. 75–94, Elsevier, New York.

Woodworth, P. L., and D. L. Blackman (2004), Evidence for systematic changes in extreme high waters since the mid-1970s, *J. Climate*, *17*, 1190–1197.

Zhang, K., B. C. Douglas, and S. P. Leatherman (2000), Twentieth-century storm activity along the U. S. east coast, *J. Climate*, *13*, 1748–1761.

K. J. Horsburgh and C. Wilson, Proudman Oceanographic Laboratory, 6 Brownlow Street, Liverpool, L3 5DA, UK. (cwi@pol.ac.uk)